

Article

Tribological Behaviors of Polycrystalline Cubic Boron Nitride Sliding against Bearing Steel in Vacuum Conditions

Fan Yang¹, Zhe Wu², Dezhong Meng^{3,4,*} , Wenbo Qin^{2,4}  and Dingshun She^{2,4}

¹ Sinounited Investment Group Corporation Limited, Beijing 101102, China; f.yang@sinowellking.com
² School of Engineering and Technology, China University of Geosciences (Beijing), Beijing 100083, China; mdz719@hotmail.com (Z.W.); qwb_strive@126.com (W.Q.); shedingshun@163.com (D.S.)
³ School of Science, China University of Geosciences (Beijing), Beijing 100083, China
⁴ Zhengzhou Institute, China University of Geosciences (Beijing), Zhengzhou 451283, China
* Correspondence: mdz604@163.com; Tel.: +86-10-8232-1062

Abstract: In order to understand the surface and interface conditions of polycrystalline cubic boron nitride (PcBN) sliding against bearing steel in vacuum environments, the effects of different loads on the tribological behaviors of PcBN and bearing steel AISI 52100 were studied deeply in a vacuum tribometer. Furthermore, the wear tracks of PcBN and the wear scars of AISI 52100 were characterized by scanning electron microscopy and energy dispersive X-ray spectroscopy. The results show that the stable coefficient of friction (CoF) of the tribopair experiences a decrease first and then an increase with the increase in loads from 2 N to 15 N. The adhesive layer increases with the increase in loads, and the formation of adhesive layer contributes to the change of CoF and wear rate of counterpart balls. The adhesive layer is formed due to the combination of high contact stress and high temperature. Meanwhile, the exfoliated cubic boron nitride grains are embedded into the adhesive layer as abrasive grains, resulting in abrasive wear. Thus, the main wear mechanisms are adhesive wear and abrasive wear.



Citation: Yang, F.; Wu, Z.; Meng, D.; Qin, W.; She, D. Tribological Behaviors of Polycrystalline Cubic Boron Nitride Sliding against Bearing Steel in Vacuum Conditions. *Coatings* **2022**, *12*, 693. <https://doi.org/10.3390/coatings12050693>

Academic Editor: Rubén González

Received: 24 April 2022

Accepted: 13 May 2022

Published: 18 May 2022

Publisher's Note: MDPI stays neutral with regard to jurisdictional claims in published maps and institutional affiliations.



Copyright: © 2022 by the authors. Licensee MDPI, Basel, Switzerland. This article is an open access article distributed under the terms and conditions of the Creative Commons Attribution (CC BY) license (<https://creativecommons.org/licenses/by/4.0/>).

Keywords: PcBN; bearing steel; tribology; vacuum condition; wear mechanisms

1. Introduction

Polycrystalline cubic boron nitride (PcBN) is sintered with cBN and binders under high pressure and high temperature. Usually, binders can be metals (Al, Co, Ti, and Ni) or ceramics (AlN, TiN, TiC, and Al₂O₃). The PcBN tool shows the advantages of high hardness, excellent wear resistance, high thermal conductivity, and chemical inertness [1–3]. It is a typical green manufacturing high-speed cutting tool and has an important application prospect in the field of space manufacturing technology [4–7]. It is proved that the friction and wear behaviors of tools and metals can be affected by the complex vacuum environment, resulting in the elusive failure modes of materials [8–10]. However, the surface and interface relationship between PcBN and metals in vacuum condition still remains elusive. Up until now, the tribological behaviors of cubic boron nitride (cBN) and its related PcBN are mainly focused on cBN films, which are famous for providing protective coatings [11,12]. It is clarified that the effects of physical and mechanical properties of cBN film with SUS 304 and TiC-coated SUS 304 on tribological behaviors are investigated in a vacuum [12]. Furthermore, the surface and interface science of PcBN and Si₃N₄ are deeply discussed. The coefficient of friction (CoF) and wear mechanisms of PcBN-Si₃N₄ tribopair show great difference in vacuum and air [13]. The transfer film results in low CoF in air while a change from sliding friction to rolling friction is presented in a vacuum. Although the tribological research of the PcBN-Si₃N₄ tribopair can provide practical guidance, the failure mode of metals still needs further investigation. Similarly to PcBN, the other famous super-hard material, diamond, and its related polycrystalline diamond composite (PDC) are well understood with respect to their tribology behaviors in vacuum and air. The CoF

between diamond and diamond can reach as high as 1.0 in vacuum, while it shows a low CoF between 0.05 and 0.15 in air [14,15]. Zhao found that the CoF of PDC in a vacuum was much higher than that in air, which was mainly due to the adhesion effect caused by the desorption of the adsorption film on the surface of the tribopair [16]. The wear mechanisms of PDC in vacuum are also dominated by environmental conditions, such as temperature, vacuum pressure, and so on [17–19]. It is well known that PcBN keeps chemical inert with metals such as Fe and Ni under high temperature, which is an important advantage compared with PDC. Therefore, taking the potential application of PcBN in the field of orbit manufacturing into consideration, it is imperative to reveal the vacuum tribological performances of PcBN sliding against metals. In the present study, we systematically developed the inner relationship between the CoF and the wear mechanisms of PcBN-AISI 52100 tribopair, which is of great significance for understanding the surface and interface relationship of PcBN and metals.

2. Materials and Methods

The PcBN produced by Zhengzhou Realy Superabrasives Co., Ltd. (Zhengzhou, China) was selected in this research. In PcBN, the content of cBN was 80%, and the main binders were AlN, CoN, and CoB. The AISI 52100 ball with a diameter of 6 mm was used in this experiment. The surface roughnesses of PcBN and AISI 52100 ball were 100–120 nm and 20–30 nm, respectively. The tribological experiments were conducted in the multifunctional space tribometer test system (MSTS-1), which was a ball-on-disk tribometer. MSTS-1 was produced by Shenyang kejing automation equipment Co., Ltd. (Shenyang, China), as shown in Figure S1 [13]. Taking the practical working conditions into consideration, the loads were 2 N, 5 N, 10 N, and 15 N. The rotation speed was suitable for the medium speed cutting range (30 mm/s), which was 100 rpm. A rotation radius of 3 mm was chosen in the tribological test. The total sliding distance was 169.56 m with a total of 30 min. PcBN and AISI 52100 balls were ultrasonically cleaned in acetone and alcohol for 15 min before the experiments. The tests were repeated three times and dates were obtained on the basis of repeated experiments. The morphologies of wear scars and wear tracks were analyzed by using a scanning electron microscope (SEM, FEI company, Hillsboro, OR, USA) and optical microscope (OLYMPUS BX51 M) (OLYMPUS, Wuxi, China) with a Nikon camera. The compositions of worn debris were characterized by an energy-dispersive X-ray spectroscope (EDS) equipped in SEM. During SEM analysis, the accelerating voltage was 15.0 kV and the spot diameter was 4.5. The Archard wear equation was used to obtain the wear rate of counter balls [20]:

$$h = R - (R^2 - r^2)^{1/2} \quad (1)$$

$$V = \pi h(3r^2 + h^2)/6 \quad (2)$$

where R (mm) is the radius of the AISI 52100 ball, r (mm) is the radius of the wear scar, and h (mm) is the height of the spherical crown:

$$W_R = V/(F_n * L) \quad (3)$$

where W_R is the wear rate per unit load and per unit distance, F_n (N) was the applied load, and L (mm) is the sliding distance.

3. Results and Discussion

Figure 1a shows the secondary electron SEM image of PcBN. It is clear that PcBN shows dense microstructure without pores. The backscattered electron SEM image of PcBN was investigated to understand the distribution of binder, as shown in Figure 1b. The darker regions correspond to cBN grains and the lighter regions correspond to binder phases. The XRD of the PcBN can be seen from reference [13], and the binder phases are AlN, CoN, and CoB. It is seen that the binder phases of PcBN are distributed discontinuously, presenting

the formation of mutual penetrating skeletons. The results indicate that the original PcBN is a homogeneous compact.

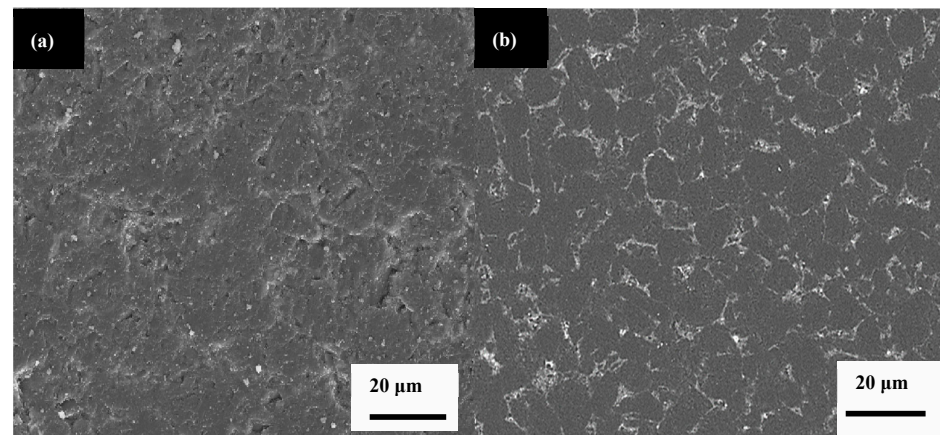


Figure 1. (a) Secondary electron SEM image of PcBN; (b) backscattered electron SEM image of PcBN.

Figure 2a presents the effect of time versus CoF during PcBN sliding against AISI 52100. It is seen that the CoFs progressively increase at the first 7 min in all loads and the break-in period finishes at around 13 min. However, the trend of CoFs in the break-in period show different in 2 N and 10 N. It may be affected by the wear mechanism of the tribopair. CoFs are mostly stable after 13 min, and they proceed to a steady-state. Figure 2b shows that the stable CoF of the tribopair decreases firstly and then increases with an increase in loads from 2 N to 15 N. The highest average CoF is 1.19 at 2 N. In addition, when the load is 10 N, the average CoF reaches the lowest value of 0.64, which is similar to CoF in air [5]. The wear rate of counterpart balls decreases with the increase in loads, showing $14.2 \times 10^{-12} \text{ mm}^3/\text{N mm}$ at 2 N and $7.6 \times 10^{-12} \text{ mm}^3/\text{N mm}$ at 15 N, as shown in Figure 2c. However, the wear volume of counterpart balls exhibit increases when adding loads. Hence, the loads exhibit an obvious influence on the friction and wear rate of PcBN-AISI 52100 tribopair. Furthermore, compared with the wear rate in air ($10^{-8} \text{ mm}^3/\text{N mm}$ in order), the wear rate in vacuum is much lower [5]. It may come from complex serious adhesion.

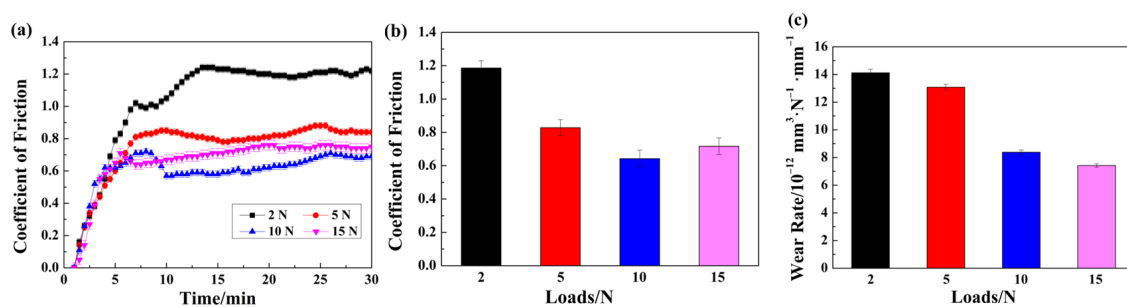


Figure 2. (a) Time dependent of CoF; (b) average CoF under different loads; (c) wear rate of AISI 52100 under different loads.

Figure 3 presents the wear morphologies of wear scars on AISI 52100 balls under different loads. Overall, it is observed that the adhesive layers are on the surface of AISI 52100 balls. In order to characterize typical features of wear scars, highly magnified SEM images were investigated on red box regions. It is seen that the small grains are embedded on the surface of wear scars, as shown in the typical pictures of Figure 3a,c inserts. The appearance of small grains is caused by the Hertz contact stress. EDS results display the high content of element B and N, which indicate the existence of cBN grains. The cBN grains act as the three-body material between the tribopairs. Thus, the main wear

mechanisms of AISI 52100 are adhesive wear and abrasive wear. Under the combination of high contact stress and friction heat, AISI 52100 metal materials with soft hardness formed an adhesive layer. In addition, the exfoliated cBN grains are embedded into the adhesive layer of the contact surface as abrasive particles, resulting in abrasive wear. Furthermore, the adhesive layer results in a downward trend of CoF and the wear rate of counterpart balls. Thus, there is a strong mutual influence on CoF and wear mechanisms, which are dominated by the loads.

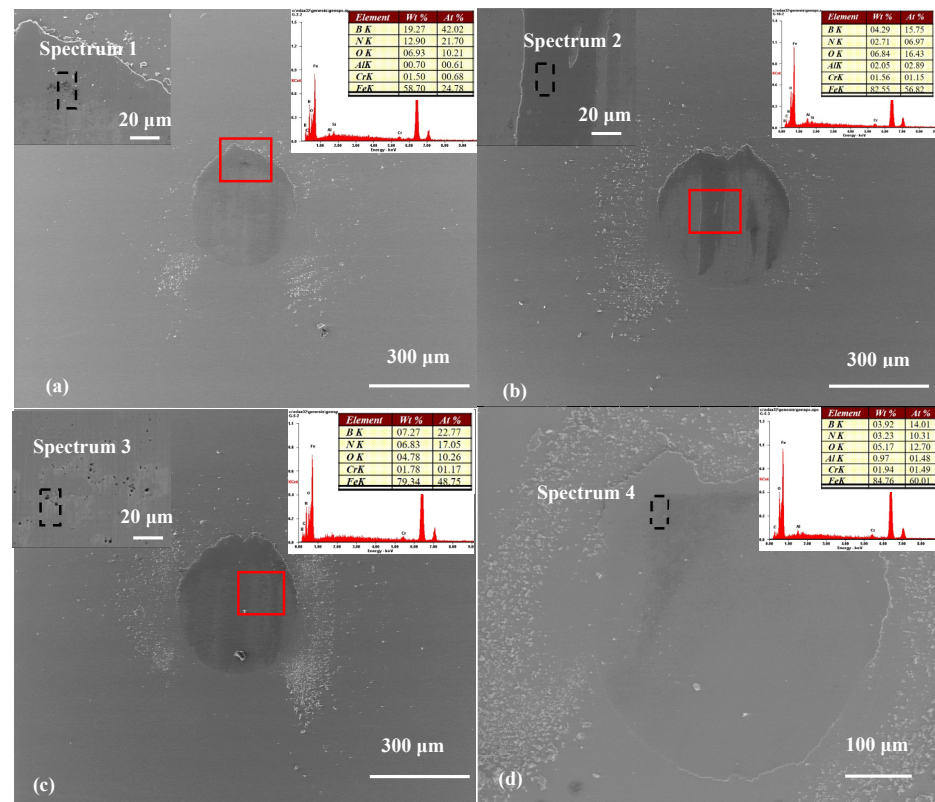


Figure 3. SEM wear morphologies of AISI 52100 under different loads: (a) 2 N; (b) 5 N; (c) 10 N; (d) 15 N. The inserts on the left of (a–c) are the high magnification of the corresponding red box positions. The EDS result on the right of (a–d) represents the elements on the black dashed box.

Figure 4 exhibits the wear morphologies of wear tracks under various loads. It can be observed that the worn debris heaps up on the edge of the wear scar, which includes the typical white adhesive layer. Furthermore, worn debris shows an increasing trend with the increase in loads. The inserts on the left of each picture indicate typical adhesive worn debris. EDS element analysis technology is used on the worn debris region to understand wear mechanisms. It is seen from the EDS results that Fe appears on the surface of adhesive layer, which comes from the counterpart ball. The adhesive layer forms due to the contact stress and the high flash temperature. Thus, the main wear mechanism is adhesive wear.

Figure 5 presents the wear mechanisms of PCBN and AISI 52100. At the early stage of sliding, the Hertz contact stress is higher than that in the final stage due to the contact area. cBN grains and binders are exfoliated. During the sliding process, the heat cumulates on the contact area since the heat transferring process is difficult in vacuum. Thus, the soft and ductile metal adheres on the surface of PcBN. Compared with the tribological behaviors in air, the adhesive wear in vacuum is more serious [5]. The results manifest that metal materials are more likely to adhere to the PcBN in vacuum and high load conditions.

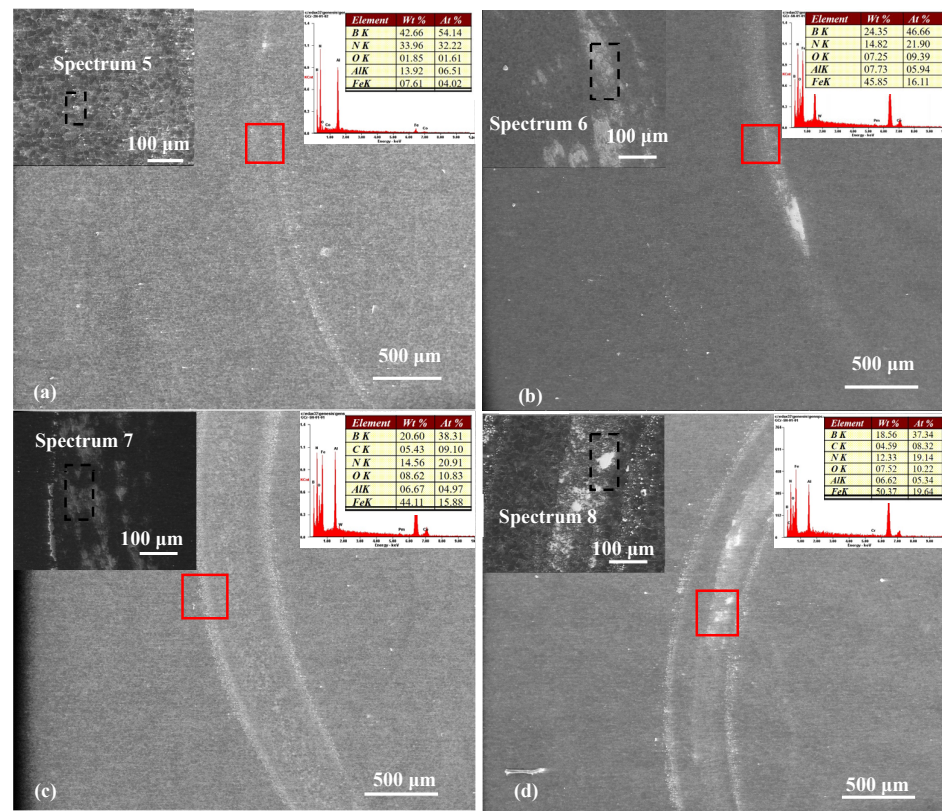


Figure 4. SEM wear morphologies of PcBN under different loads: (a) 2 N; (b) 5 N; (c) 10 N; (d) 15 N. The inserts on the left of (a–d) are the high magnification of the corresponding red box positions. The EDS result on the right of (a–d) represent the elements on the black dashed box.

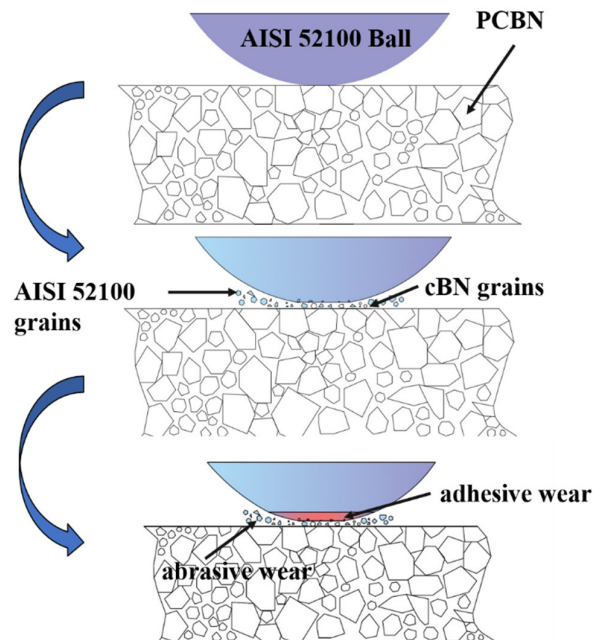


Figure 5. Wear mechanisms of PcBN and AISI 52100.

4. Conclusions

In this paper, the tribological behaviors of PcBN and AISI 52100 in vacuum environment were fully investigated. The main conclusions are as follows.

(1) The tribological behaviors of PcBN and AISI 52100 tribopairs in vacuum environments are affected by loads. CoF and wear rate decrease with the increase in loads. The appearance of the adhesive layer leads to a decrease in CoF and wear rate.

(2) The wear forms of PcBN-AISI 52100 tribopair are mainly adhesive wear and abrasive wear. With the increase in loads, adhesive wear is dominated the surface and interface conditions. The accumulation of friction heat and the high load are responsible for the adhesive layer. The abrasive wear is ascribed to falling-off cBN particles, which act as the hard phase on friction surfaces.

Supplementary Materials: The following supporting information can be downloaded at: <https://www.mdpi.com/article/10.3390/coatings12050693/s1>, Figure S1: The MSTS-1 Multifunctional Vacuum Friction and Wear Testing Machine.

Author Contributions: Conceptualization, methodology, validation, and formal analysis, F.Y.; investigation and data curation, Z.W.; resources, D.M.; writing—original draft preparation, F.Y. and Z.W.; writing—review and editing, D.M.; supervision, W.Q.; project administration, D.S.; funding acquisition, D.M. All authors have read and agreed to the published version of the manuscript.

Funding: This work was financially supported by Beijing Natural Science Foundation (3214052), Fundamental Research Funds for the Central Universities (2652019109), National Natural Science Foundation of China (51472224), and China Postdoctoral Science Foundation (2020TQ0300).

Institutional Review Board Statement: Not applicable.

Informed Consent Statement: Not applicable.

Data Availability Statement: Not applicable.

Conflicts of Interest: The authors declare no conflict of interest.

References

1. Zhu, Y.J.; Ding, W.F.; Yu, T.Y.; Xu, J.H.; Fu, Y.C.; Su, H.H. Investigation on stress distribution and wear behavior of brazed polycrystalline cubic boron nitride superabrasive grains: Numerical simulation and experimental study. *Wear* **2017**, *376*–377, 1234–1244. [[CrossRef](#)]
2. Bushlya, V.M.; Gutnichenko, O.A.; Zhou, J.M.; Ståhl, J.E.; Gunnarsson, S. Tool wear and tool life of PCBN, binderless CBN and WBN-CBN tools in continuous finish hard turning of cold work tool steel. *J. Superhard Mater.* **2014**, *36*, 49–60. [[CrossRef](#)]
3. Liu, X.L.; Wen, D.H.; Li, Z.J.; Xiao, L.; Yan, F.G. Experimental study on hard turning hardened GCr15 steel with PCBN tool. *J. Mater. Process. Technol.* **2002**, *129*, 217–221. [[CrossRef](#)]
4. Rao, Z.W.; Xiao, G.D.; Zhao, B.; Zhu, Y.J.; Ding, W.F. Effect of wear behaviour of single mono- and poly-crystalline cBN grains on the grinding performance of Inconel 718. *Ceram. Int.* **2021**, *47*, 17049–17056. [[CrossRef](#)]
5. Meng, D.; Zhao, Y.; Yue, W.; Wu, Z.; Cui, J.; Qin, W.; Wang, C. Thermal effects on tribological behaviors of polycrystalline cubic boron nitride. *Ceram. Int.* **2021**, *47*, 7117–7125. [[CrossRef](#)]
6. Gao, H.; Liu, X.; Chen, Z. Cutting performance and wear/damage characteristics of PCBN tool in hard milling. *Appl. Sci.* **2019**, *9*, 772. [[CrossRef](#)]
7. Dogra, M.; Sharma, V.S.; Sachdeva, A.; Suri, N.M.; Dureja, J.S. Tool wear, chip formation and workpiece surface issues in CBN hard turning: A review. *Int. J. Precis. Eng. Man.* **2010**, *14*, 341–358. [[CrossRef](#)]
8. Prozhega, M.V.; Kharkov, M.M.; Reschikov, E.O.; Rykunov, G.I.; Kaziev, A.V.; Kukushkina, M.S.; Kolodko, D.V.; Stepanova, T.V. Estimation of MoS₂ Coating Performance on Bronze and Steel in Vacuum at High Temperatures. *Coatings* **2022**, *12*, 125. [[CrossRef](#)]
9. Kang, J.; Wang, C.; Wang, H.; Xu, B.; Liu, J.; Li, G. Research on tribological behaviors of composite Zn/ZnS coating under dry condition. *Appl. Surf. Sci.* **2012**, *258*, 1940–1943. [[CrossRef](#)]
10. She, D.; Yue, W.; Fu, Z.; Gu, Y.; Wang, C.; Liu, J. The effect of nitriding temperature on hardness and microstructure of die steel pre-treated by ultrasonic cold forging technology. *Mater. Design* **2013**, *49*, 392–399. [[CrossRef](#)]
11. Linss, V.; Rodil, S.E.; Reinke, P.; Garnier, M.G.; Oelhafen, P.; Kreissig, U.; Richter, F. Bonding characteristics of DC magnetron sputtered B–C–N thin films investigated by Fourier-transformed infrared spectroscopy and X-ray photoelectron spectroscopy. *Thin Solid Films* **2004**, *467*, 76–87. [[CrossRef](#)]
12. Yu, Z.M.; Inagawa, K.; Jin, Z.J. Tribological properties of c-BN coatings in vacuum at high temperature. *Surf. Coat. Technol.* **1994**, *70*, 147–150. [[CrossRef](#)]

13. Cui, J.; Meng, D.; Wu, Z.; Qin, W.; She, D.; Kang, J.; Zhang, R.; Wang, C.; Yue, W. Tribological behaviors of polycrystalline cubic boron nitride sliding against silicon nitride in air and vacuum conditions. *Ceram. Int.* **2022**, *48*, 363–372. [[CrossRef](#)]
14. Tzeng, Y. Very low friction for diamond sliding on diamond in water. *Appl. Phys. Lett.* **1993**, *63*, 3586–3588. [[CrossRef](#)]
15. Grillo, S.E.; Field, J.E. The friction of natural and CVD diamond. *Wear* **2003**, *254*, 945–949. [[CrossRef](#)]
16. Zhao, Y.; Yue, W.; Lin, F.; Wang, C.; Wu, Z. Friction and wear behaviors of polycrystalline diamond under vacuum conditions. *Int. J. Refract. Met. Hard Mater.* **2015**, *50*, 43–52. [[CrossRef](#)]
17. Sha, X.; Yue, W.; Zhao, Y.; Lin, F.; Wang, C. Effect of sliding mating materials on vacuum tribological behaviors of sintered polycrystalline diamond. *Int. J. Refract. Met. Hard Mater.* **2016**, *54*, 116–126. [[CrossRef](#)]
18. Sha, X.; Yue, W.; Wang, C. Vacuum pressure dependence of the tribological behaviors of sintered polycrystalline diamond sliding against silicon nitride. *Int. J. Refract. Met. Hard Mater.* **2016**, *61*, 30–39. [[CrossRef](#)]
19. Liu, Y.; Yue, W.; Qin, W.; Wang, C. Improved vacuum tribological properties of sintered polycrystalline diamond compacts treated by high temperature annealing. *Carbon* **2017**, *124*, 651–661. [[CrossRef](#)]
20. Archard, J.F. Contact and rubbing of flat surfaces. *J. Appl. Phys.* **1953**, *24*, 981–988. [[CrossRef](#)]